Spatio-colour Asplünd 's metric and Logarithmic Image Processing for Colour Images (LIPC)

Guillaume Noyel, Michel Jourlin

Spatio-colour Asplünd's metric and Logarithmic Image Processing for Colour Images (LIPC)

Guillaume Noyel[1] and Michel Jourlin[1,2]

[1] International Prevention Research Institute, 95 cours Lafayette, 69006 Lyon, France
[2] Lab. H. Curien, UMR CNRS 5516, 18 rue Pr. B. Lauras, 42000 St-Etienne, France
www.i-pri.org

Abstract. Asplünd's metric, which is useful for pattern matching, consists in a double-sided probing, i.e. the over-graph and the sub-graph of a function are probed jointly. This paper extends the Asplünd's metric we previously defined for colour and multivariate images using a marginal approach (i.e. component by component) to the first spatio-colour Asplünd's metric based on the vectorial colour LIP model (LIPC). LIPC is a non-linear model with operations between colour images which are consistent with the human visual system. The defined colour metric is insensitive to lighting variations and a variant which is robust to noise is used for colour pattern matching.

Keywords: Asplünd's metric, spatio-colour metric, colour Logarithmic Image Processing, double-sided probing, colour pattern recognition

1 Introduction

The Asplünd's metric initially defined for binary shapes [1, 4] has been extended to grey-scale images by Jourlin et al. [6, 7] and to colour and multivariate images in the LIP framework by Noyel et al. [13]. It consists in probing a function by two homothetic template functions, i.e. the probes which are computed by the LIP multiplication.

The Logarithmic Image Processing (LIP) model initially defined for grey level images by Jourlin et al. in [8, 9] is perfectly suited for images acquired by transmitted light (i.e. when the observed object is located between the source and the sensor) and by reflected light because of its consistency with the Human Vision [3]. In the LIP framework, the results of operations such as addition, subtraction or multiplication by a scalar stay in the bounded domain of images ([0...255] for 8-bits images). The necessity to analyse together the channels of the colour images (i.e. by a vectorial analysis) has led to the introduction of the Logarithmic Image Processing for Colour images (LIPC) by Jourlin et al. in [5].

The LIP Asplünd's metric was defined in [13] in a marginal way (i.e. channel by channel). In this paper, our contribution is to extend this metric by using the spatio-colour properties [11, 12] of the colour LIPC framework.

After some prerequisites about the colour LIPC model and about the marginal LIP Asplünd's metric, we will define a spatio-colour Asplünd's metric in the

LIPC framework. Then we will perform spatio-colour pattern matching which is robust to noise. Examples will illustrate the definitions.

2 Prerequisites

2.1 LIPC model

A colour image $\mathbf{f}$, defined on a domain $D \subset \mathbb{R}^N$, with values in $\mathcal{T}^3 = [0, M[^3$, $M \in \mathbb{R}$, is written:

$$\mathbf{f} : \begin{cases} D \rightarrow & \mathcal{T}^3 = [0, M[^3 \\ x \rightarrow \mathbf{f}(x) = & (f_R(x), f_G(x), f_B(x)) \end{cases} \tag{1}$$

f_R , f_G , f_B are the red, green and blue channels (i.e. components) of $\mathbf{f}$, $\mathbf{f}(x)$ is a vector-pixel and x is the spatial coordinate of the vector-pixel. The real value M is equal to $2^8 = 256$ for 8 bits images. Given P the number of pixels, the matrix $\mathbf{F}$ of $E \rightarrow \mathcal{T}$, $E = 3 \times P$, associated to the image $\mathbf{f}$ is written:

$$\mathbf{F} = \begin{bmatrix} f_R(x_1)\ f_R(x_2)\ ...\ f_R(x_P) \\ f_G(x_1)\ f_G(x_2)\ ...\ f_G(x_P) \\ f_B(x_1)\ f_B(x_2)\ ...\ f_B(x_P) \end{bmatrix} \tag{2}$$

To make easier the comments, the word "image" designates both the matrix $\mathbf{F}$ and the image $\mathbf{f}$. The image space for 24-bits images $\mathbf{F}$ is written $\mathcal{I}^3$.

A colour image is a particular case of a multivariate image defined as $\mathbf{f}_\lambda : D \rightarrow \mathcal{T}^L$, where $L \in \mathbb{N}$ is the number of channels [11, 12].

As for the grey-level LIP, the colour LIPC framework is based on colour transmittance [5]. It is valid for transmitted and reflected images [3]. It models the human perceptual system approach by taking into account: *i*) the sensitivity of the human eye in the visible domain characterised by colour matching functions of Stiles and Burch (1959) [14] and *ii*) the spectral distribution of light with the D65 illuminant [14].

In the LIPC framework, the transmittance of the sum of two images $\mathbf{T}_{\mathbf{F} \triangle_c \mathbf{G}}$ is equal to the product of their transmittances $\mathbf{T}_\mathbf{F}$ and $\mathbf{T}_\mathbf{G}$: $\mathbf{T}_{\mathbf{F} \triangle_c \mathbf{G}} = \mathbf{T}_\mathbf{F} * \mathbf{T}_\mathbf{G}$. The symbol of the LIPC addition is $\triangle_c$ and $*$ represents the element-wise multiplication [5]. The addition of two images $\mathbf{F}, \mathbf{G} \in \mathcal{I}^3$ is:

$$\mathbf{F} \triangle_c \mathbf{G} = \acute{\mathbf{K}}^{-1} \acute{\mathbf{U}} (\acute{\mathbf{U}}^{-1} \acute{\mathbf{K}} \mathbf{F} * \acute{\mathbf{U}}^{-1} \acute{\mathbf{K}} \mathbf{G}). \tag{3}$$

$\acute{\mathbf{K}}$ and $\acute{\mathbf{U}}$ are real matrices of size 3×3 corresponding to the LIPC mixing model [3]. From the LIPC addition, a multiplication by a scalar $\alpha \in \mathbb{R}$ has been defined:

$$\alpha \triangle_c \mathbf{F} = \acute{\mathbf{K}}^{-1} \acute{\mathbf{U}} (\acute{\mathbf{U}}^{-1} \acute{\mathbf{K}} \mathbf{F})^\alpha. \tag{5}$$

[3] With colour matching functions of Stiles and Burch (1959) and D65 illuminant [5], matrices $\acute{\mathbf{K}}$ and $\acute{\mathbf{U}}$ equal to:

$$\acute{\mathbf{U}} = \begin{bmatrix} 25.0440 & 53.1416 & 176.8144 \\ 21.3002 & 185.9744 & 47.7254 \\ 229.2474 & 19.9944 & 5.7583 \end{bmatrix} \acute{\mathbf{K}} = \begin{bmatrix} 0.6991 & 0.2109 & 0.0899 \\ 0.1947 & 0.8002 & 0.0049 \\ 0.0681 & 0.0002 & 0.9315 \end{bmatrix} \tag{4}$$

The space $(\mathcal{I}^3, \triangleq_c, \triangleq_c)$ is the positive cone of a vector space with robust mathematical properties.

Physical interpretation [5]: the LIPC addition corresponds to the superposition of two semi-transparent layers. A LIPC multiplication by a scalar $\alpha \in]0,1[$ brightens the result by suppressing layers, while a scalar $\alpha \in]1,+\infty[$ darkens the result by superimposing α times the image on itself.

2.2 Marginal Asplünd's metric for colour and multivariate images

In [13], an Asplünd's metric between colour images was defined with the LIP model by using marginal approach (i.e. channel by channel) [11, 12] .

Definition 1. *The Asplünd's metric (with LIP multiplication) between two colour images* $\mathbf{f}$ *and* $\mathbf{g}$ *on a region* $Z \subset D$ *is*

$$d^{\triangleq}_{As,Z}(\mathbf{f},\mathbf{g}) = \ln(\lambda/\mu) \tag{6}$$

with $\lambda = \inf\{k, \forall x \in Z, k \triangleq g_R(x) \geq f_R(x), k \triangleq g_G(x) \geq f_G(x), k \triangleq g_B(x) \geq f_B(x)\}$
and $\mu = \sup\{k, \forall x \in Z, k \triangleq g_R(x) \leq f_R(x), k \triangleq g_G(x) \leq f_G(x), k \triangleq g_B(x) \leq f_B(x)\}$.

In particular, by the property of the distance $d^{\triangleq}_{As,Z}(\mathbf{f},\mathbf{g}) = d^{\triangleq}_{As,Z}(\mathbf{g},\mathbf{f})$.

3 Asplünd's metric defined in the Logarithmic Image Processing Colour (LIPC) framework

Given two colours $C_1 = (r_1, g_1, b_1)$, $C_2 = (r_2, g_2, b_2) \in \mathcal{T}^3$, as we are only looking for lower and upper bounds, a marginal order [2] is used: $C_1 \geq C_2 \Leftrightarrow \{r_1 \geq r_2$ and $g_1 \geq g_2$.

Definition 2. *Given two colours* C_1, $C_2 \in \mathcal{T}^3$, *their Asplünd's distance (with LIPC multiplication) is equal to:*

$$d^{\triangleq_c}_{As}(C_1, C_2) = \ln(\mu/\lambda) \tag{7}$$

$\lambda = \inf_k \{k \triangleq_c C_2 \geq C_1\}$ *and* $\mu = \sup_k \{k \triangleq_c C_2 \leq C_1\}$.

Strictly speaking, $d^{\triangleq_c}_{As}$ is a metric if the colours C_n are replaced by their equivalence classes $\tilde{C}_n = \left\{C \in \mathcal{T}^3 / \exists \alpha \in \mathbb{R}^+, \ \ \alpha \triangleq_c C = C_n\right\}$.

Comment: in eq. 7 contrary to the Asplünd's distance (with LIP multiplication) defined in [13], we have $\lambda \leq \mu$ because, by definition of the colour LIPC model the scales are inverted as compared to the grey LIP model [5].

Colour metrics (with LIPC multiplication) between two colour images $\mathbf{f}$ and $\mathbf{g}$ may be defined as the sum (d_1 metric) or the supremum (d_∞) of $d^{\triangleq_c}_{As}(C_1, C_2)$ on the region of interest $Z \subset D$ of cardinal $\#Z$

$$\begin{array}{l} d^{\triangleq_c}_{1,Z}(\mathbf{f},\mathbf{g}) \ = \frac{1}{\#Z} \sum_{x \in Z} d^{\triangleq_c}_{As}(\mathbf{f}(x),\mathbf{g}(x)) \\ d^{\triangleq_c}_{\infty,Z}(\mathbf{f},\mathbf{g}) = \ \sup_{x \in Z} d^{\triangleq_c}_{As}(\mathbf{f}(x),\mathbf{g}(x)) \end{array} \tag{8}$$

The Asplünd's metric can be extended to colour functions.

Definition 3. *The colour Asplünd's metric (with LIPC multiplication) between two colour images* $\mathbf{f}$ *and* $\mathbf{g}$ *on a region* $Z \subset D$ *is*

$$d^{\triangle_c}_{As,Z}(\mathbf{f},\mathbf{g}) = \ln(\mu/\lambda) \tag{9}$$

with $\lambda = \inf_k \{\forall x \in Z, k \triangle_c \mathbf{g}(x) \geq \mathbf{f}(x)\}$ *and* $\mu = \sup_k \{\forall x \in Z, k \triangle_c \mathbf{g}(x) \leq \mathbf{f}(x)\}$.

In fig. 1, the Asplünd's metric has been computed between the colour probe $\mathbf{g}$ and the colour function $\mathbf{f}$ on their definition domain D.

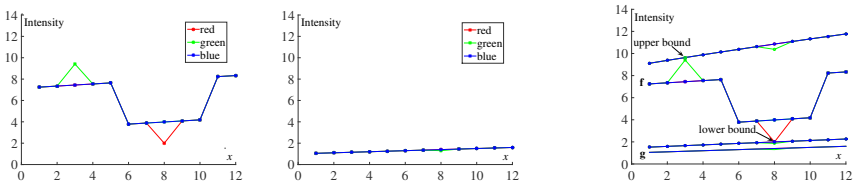

(a) Colour function $\mathbf{f}$ (b) Colour probe $\mathbf{g}$ (c) Lower (μ) and upper (λ) bounds

Fig. 1. Computation of the Asplünd's distance between two colour functions $d^{\triangle_c}_{As,D}(\mathbf{f},\mathbf{g}) = 0.43$. Each colour channel is represented by a line of the same colour.

Comment: the lower (resp. upper) bound $\mu \triangle_c \mathbf{g}$ (resp. $\lambda \triangle_c \mathbf{g}$) may not be equal to any point of the function $\mathbf{f}$ but strictly less (or greater) than the function. Indeed, one can demonstrate that the following assertion is verified: "given $\mathbf{C}_0 \in \mathcal{T}^3, \forall C \in \mathcal{T}^3, \nexists \lambda \in \mathbb{R}^+ / \lambda \triangle_c C_0 = C$".

The metric $d^{\triangle_c}_{As,Z}$ can be adapted to local processing with a colour template image (i.e. the probe) $\mathbf{t}$ defined on a spatial support $D_t \subset D$. For each point $x \in D$, the distance $d^{\triangle_c}_{As,D_t}(\mathbf{f}_{|D_t(x)}, \mathbf{t})$ is computed on the neighbourhood $D_t(x)$ centred in x where $\mathbf{f}_{|D_t(x)}$ is the restriction of $\mathbf{f}$ to $D_t(x)$.

Definition 4. *Given a colour image* $\mathbf{f}$ *defined on* D *with values in* $\mathcal{T}^3$, $\left(\mathcal{T}^3\right)^D$, *a colour probe* $\mathbf{t}$ *defined on* D_t *with values in* $\mathcal{T}^3$, $\left(\mathcal{T}^3\right)^{D_t}$ *and* $D_t(x)$ *the neighbourhood* D_t *centred in* $x \in D$, *the map of Asplünd's distances (with* $\triangle_c$*) is:*

$$As^{\triangle_c}_{\mathbf{t}}\mathbf{f} : \begin{cases} \left(\mathcal{T}^3\right)^D \times \left(\mathcal{T}^3\right)^{D_t} \to & \left(\mathbb{R}^+\right)^D \\ (\mathbf{f},\mathbf{t}) \to As^{\triangle_c}_{\mathbf{t}}\mathbf{f}(x) = d^{\triangle_c}_{As,D_t}(\mathbf{f}_{|D_t(x)}, \mathbf{t}) & \end{cases} \tag{10}$$

In figure 2, the map of Asplünd's distances is computed between a colour function and a colour probe. The minima of the map corresponds to the location of a pattern which is similar to the probe.

Asplünd's distance is sensitive to noise because the probe lays on regional extrema that may be caused by noise (Figure 1). In [7, 13], definitions of Asplünd's distance with a tolerance on the extrema have been introduced. In this paper,

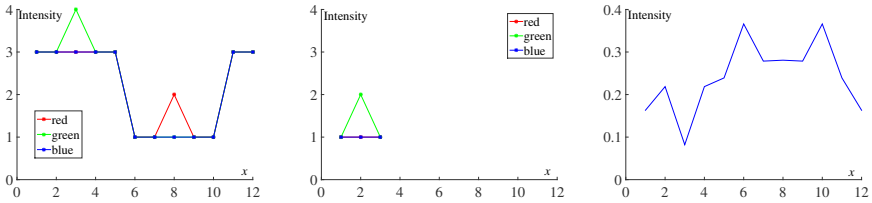

(a) Colour function $\mathbf{f}$ (b) Colour probe $\mathbf{t}$ (c) Map of Asplünd's distance $As_{\mathbf{t}}^{\triangle_c}\mathbf{f}$

Fig. 2. (c) Map of the Asplünd's distance $As_{\mathbf{t}}^{\triangle_c}\mathbf{f}$ between a colour function and a colour probe. (a) and (b) Each colour channel is represented by a line of the same colour.

we extend this definition for colour images with LIPC model using the same approach as in [13].

To reduce the sensitivity of Asplünd's distance to the noise, there exists a metric defined in the context of "Measure Theory" named the Measure metric or the M-metric. The image being digitized, the number of pixels lying in D is finite, therefore the "measure" of a subset of D is linked to the cardinal of this subset, for example the percentage P of its elements related to D (or a region of interest $R \subset D$). In this case, we are looking for a subset D' of D, such that $\mathbf{f}_{|D'}$ and $\mathbf{g}_{|D'}$ are neighbours for Asplünd's metric and the complementary set $D \setminus D'$ of D' related to D is small sized when compared to D. This last condition can be written as: $P(D \setminus D') = \frac{\#(D \setminus D')}{\#D} \leq p$ where p represents an acceptable percentage and $\#D$ the number of elements in D.

Given ϵ a small positive real number, the neighbourhood of function $\mathbf{f}$ is

$$N_{P,d_{As},\epsilon,p}(\mathbf{f}) = \left\{ \mathbf{g} \setminus \exists D' \subset D, d_{As,D'}^{\triangle_c}(\mathbf{f}_{|D'}, \mathbf{g}_{|D'}) < \epsilon \text{ and } \frac{\#(D \setminus D')}{\#D} \leq p \right\} \tag{11}$$

As in [5, 13], the closest points of the probe to the function are discarded. In figure 3, a tolerance of $p = 20\%$ is used to discard two points. The Asplünd's distance decreases from $d_{As,D}^{\triangle_c}(\mathbf{f}, \mathbf{g}) = 0.43$ to $d_{As,D,p=20\%}^{\triangle_c}(\mathbf{f}, \mathbf{g}) = 0.21$.

A map of Asplünd's distances (with $\triangle_c$) can be defined.

Definition 5. *Given a colour image* $\mathbf{f}$ *of* $\left(\mathcal{T}^3\right)^D$*, a colour probe* $\mathbf{t}$ *of* $\left(\mathcal{T}^3\right)^{D_t}$ *and a tolerance* $p \in [0, 1]$*, the map of Asplünd's distances with a tolerance is:*

$$As_{\mathbf{t},p}^{\triangle_c}\mathbf{f} : \begin{cases} \left(\mathcal{T}^3\right)^D \times \left(\mathcal{T}^3\right)^{D_t} \to & \mathbb{R}^{+D} \\ (\mathbf{f}, \mathbf{t}) \to & As_{\mathbf{t},p}^{\triangle_c}\mathbf{f}(x) = d_{As,D_t,p}^{\triangle_c}(\mathbf{f}_{|D_t(x)}, \mathbf{t}) \end{cases} \tag{12}$$

$D_t(x)$ is the neighbourhood D_t centred in $x \in D$.

Examples illustrate the results.

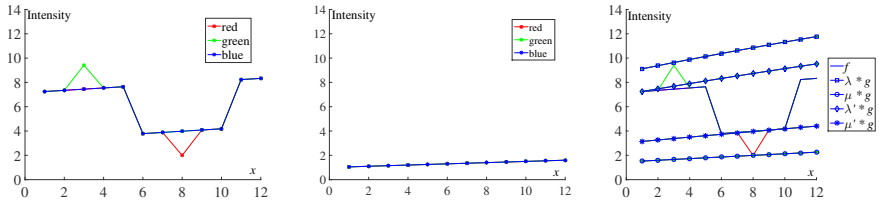

(a) Colour function $\mathbf{f}$ (b) Colour probe $\mathbf{g}$ (c) Lower and upper bounds, $p = 20\%$

Fig. 3. Colour Asplünd's distance with a tolerance of $p = 20\%$. (μ, λ) are the scalars multiplying the probe without tolerance. (μ', λ') are the scalars multiplying the probe with tolerance.

4 Examples and applications

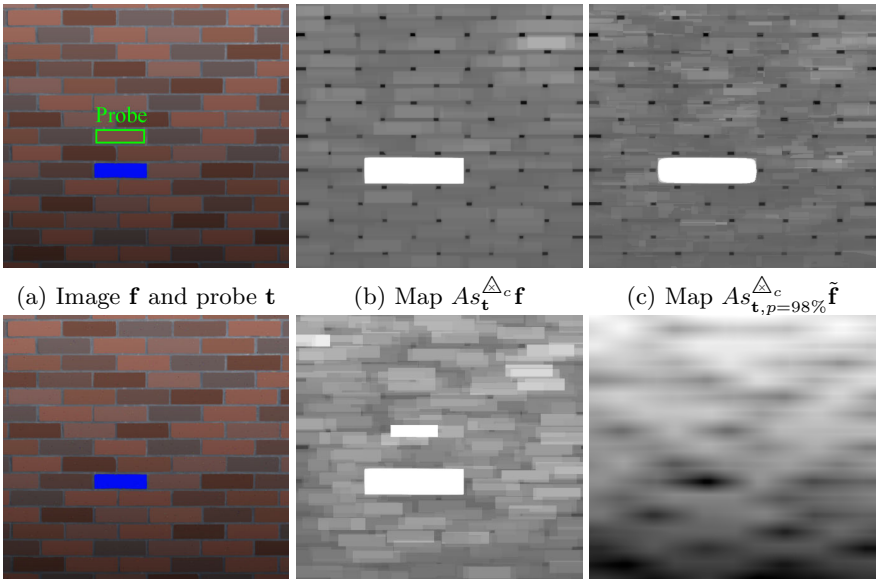

(a) Image $\mathbf{f}$ and probe $\mathbf{t}$ (b) Map $As_{\mathbf{t}}^{\triangle_c}\mathbf{f}$ (c) Map $As_{\mathbf{t},p=98\%}^{\triangle_c}\tilde{\mathbf{f}}$

(d) Noisy image $\tilde{\mathbf{f}}$ (e) Map $As_{\mathbf{t}}^{\triangle_c}\tilde{\mathbf{f}}$ (f) Correlation map

Fig. 4. Maps of Asplünd's distances without tolerance $As_{\mathbf{t}}^{\triangle_c}\tilde{\mathbf{f}}$ and with $As_{\mathbf{t},p}^{\triangle_c}\tilde{\mathbf{f}}$. $\tilde{\mathbf{f}}$ image with a white noise ($\sigma^2 = 2.6$, spatial density 1%). (e) Correlation map.

In figure 4, our aim is to find bricks of homogeneous colour inside a colour image of a brick wall with one blue brick. Usingt the image without noise $\mathbf{f}$, the regional minima of the map $As_{\mathbf{t}}^{\triangle_c}\mathbf{f}$ (fig. 4 b) correspond to the locations which are similar to the probe (with the Asplünd's distance). The distance is

inaccurate to find the position of the blue brick (large maxima) because it is sensitive to the colour of the probe. In the image with noise $\tilde{\mathbf{f}}$ (Gaussian white noise of variance 2.6 and spatial density of 1%), the map without tolerance $As^{\triangle_c}_{\mathbf{t}}\tilde{\mathbf{f}}$ is more sensitive to noise (fig. 4 e) while the map with tolerance $As^{\triangle_c}_{\mathbf{t},p}\tilde{\mathbf{f}}$ is less (fig 4 c). Indeed, the minima are preserved into the map with tolerance (fig. 4 c) compared to the map without (fig. 4 e). The minima can be extracted using standard operations of mathematical morphology [10, 15]. Importantly, all the maps of Asplünd's distances are insensitive to the vertical lighting drift. Moreover, a correlation map is useless to find the location of the bricks (fig. 4 f).

In figure 5, two images of the same scene, a bright image $\mathbf{f}$ and a dark image $\tilde{\mathbf{f}}$, are acquired with two different exposure times. The probe $\mathbf{t}$ is extracted in the bright image and used to compute the map of Asplünd's distance $As^{\triangle_c}_{\mathbf{t}}\tilde{\mathbf{f}}$ in the darker image. By finding the minima of the map, all the balls are detected and their contours are added to the image of figure 5 (b). One can notice that the Asplünd's distance is very robust to the lighting variations.

(a) Initial image $\mathbf{f}$ and probe $\mathbf{t}$ (b) Dark image $\tilde{\mathbf{f}}$ Balls detected (c) Map $As^{\triangle_c}_{\mathbf{t}}\tilde{\mathbf{f}}$

Fig. 5. Detection of coloured balls on a dark image $\tilde{\mathbf{f}}$ with a probe $\mathbf{t}$ extracted in the bright image $\mathbf{f}$. (a) The border of the probe $\mathbf{t}$ is coloured in white.

5 Conclusion and perspectives

A new spatio-colour Asplünd's distance based on colour LIPC model has been defined. It is a true colour (i.e. vectorial) metric based on a colour model consistent with the human visual system. It is also consistent with the previous properties given in [7, 13]. An extension of this metric robust to noise has been presented and illustrated on pattern recognition examples. This double-sided

probing distance is efficient for colour pattern matching and performs better than traditional correlation methods. In future work, we will evaluate in details the properties of this colour distance on practical applications (e.g. in medical, remote sensing or industrial images). We will compare it to the marginal colour Asplünd's distance and we will study the links between Asplünd's probing and mathematical morphology.

References

1. Asplünd, E.: Comparison between plane symmetric convex bodies and parallelograms. Mathematica Scandinavica 8, 171–180 (1960)
2. Barnett, V.: The ordering of multivariate data. Journal of the Royal Statistical Society. Series A (General) 139(3), 318–355 (1976)
3. Brailean, J., Sullivan, B., Chen, C., Giger, M.: Evaluating the EM algorithm for image processing using a human visual fidelity criterion. In: Acoustics, Speech, and Signal Processing, 1991. ICASSP-91., 1991 International Conference on. pp. 2957–2960 vol.4 (Apr 1991)
4. Grünbaum, B.: Measures of symmetry for convex sets. In: Proceedings of Symposia in Pure Mathematics. pp. 233–270 vol.7 (1963)
5. Jourlin, M., Breugnot, J., Itthirad, F., Bouabdellah, M., Closs, B.: Chapter 2 - Logarithmic image processing for color images. In: Hawkes, P.W. (ed.) Advances in Imaging and Electron Physics, vol. 168, pp. 65 – 107. Elsevier (2011)
6. Jourlin, M., Carré, M., Breugnot, J., Bouabdellah, M.: Chapter 7 - Logarithmic image processing: Additive contrast, multiplicative contrast, and associated metrics. In: Hawkes, P.W. (ed.) Advances in Imaging and Electron Physics, vol. 171, pp. 357 – 406. Elsevier (2012)
7. Jourlin, M., Couka, E., Abdallah, B., Corvo, J., Breugnot, J.: Asplünd's metric defined in the logarithmic image processing (LIP) framework: A new way to perform double-sided image probing for non-linear grayscale pattern matching. Pattern Recognition 47(9), 2908 – 2924 (2014)
8. Jourlin, M., Pinoli, J.: A model for logarithmic image processing. Journal of Microscopy 149(1), 21–35 (1988)
9. Jourlin, M., Pinoli, J.: Logarithmic image processing: The mathematical and physical framework for the representation and processing of transmitted images. In: Hawkes, P.W. (ed.) Advances in Imaging and Electron Physics, vol. 115, pp. 129 – 196. Elsevier (2001)
10. Matheron, G.: Eléments pour une théorie des milieux poreux. Masson, Paris (1967)
11. Noyel, G., Angulo, J., Jeulin, D.: Morphological segmentation of hyperspectral images. Image Analysis & Stereology 26(3) (2007)
12. Noyel, G., Angulo, J., Jeulin, D., Balvay, D., Cuenod, C.A.: Multivariate mathematical morphology for DCE-MRI image analysis in angiogenesis studies. Image Analysis & Stereology 34(1), 1–25 (2014)
13. Noyel, G., Jourlin, M.: Asplünd's metric defined in the logarithmic image processing (LIP) framework for colour and multivariate images. In: Image Processing (ICIP), 2015 IEEE International Conference on. pp. 3921–3925 (Sept 2015)
14. Schanda, J.: Colorimetry: Understanding the CIE System. John Wiley & Sons, Inc. (2007)
15. Serra, J., Cressie, N.: Image analysis and mathematical morphology: Vol. 1. Academic Press, London (1982)